

Crystallographic aspects of $L1_0$ magnetic materials

David E. Laughlin^{a,b}, Kumar Srinivasan^{a,b,1}, Mihaela Tanase^{b,c,*}, Lisha Wang^{a,2}

^a Department of Materials Science and Engineering, Carnegie Mellon University, Pittsburgh, PA 15213, United States

^b Data Storage Systems Center, Carnegie Mellon University, Pittsburgh, PA 15213, United States

^c Department of Physics, 5000 Forbes Ave., Carnegie Mellon University, Pittsburgh, PA 15213, United States

Received 3 December 2004; received in revised form 19 February 2005; accepted 21 April 2005

Available online 25 May 2005

Abstract

In this paper we present an overview of various features of the structure of $L1_0$ magnetic phase. We discuss the various microstructural features which occur in these materials due to the changes in symmetry (translational and orientational domains) as well as the relationship between the crystal symmetry and features such as the thermodynamic order of the disorder to order phase transition. We also show the various ways that the magnetic moments of the elements align themselves in these alloys producing ferromagnetic and antiferromagnetic materials. Finally we discuss the way that the atomic order, composition and magnetic order affect the Curie temperatures of the FePd $L1_0$ alloys.

© 2005 Acta Materialia Inc. Published by Elsevier Ltd. All rights reserved.

Keywords: Symmetry; Order–disorder; Domains; $L1_0$; Crystallography

1. Introduction

Because of their large magnetocrystalline anisotropy energies, $L1_0$ magnetic alloys may play an important role in future ultra-high density magnetic recording media. These alloys are very different from the Co-based hexagonal close-packed alloys utilized for the last two decades or so, in that they are tetragonal in symmetry and are atomically ordered structures. In this paper some of the fundamental aspects of the crystallography of the $L1_0$ structure will be explored. In particular we examine the various kinds of domains that can form in materials with these structures and present some mea-

surements of the Curie temperature for FePd alloys in both the face-centered cubic (fcc) and $L1_0$ states.

2. Crystallographic information

The fcc and $L1_0$ structures are shown in Fig. 1. The fcc structures have all their faces and their corner sites occupied by the same atoms, or in the case of an alloy, the probability of each site being occupied by a specific type of atom is the same. $L1_0$ is a crystallographic derivative structure of the fcc structure and has two of the faces occupied by one type of atom and the corner and the other face occupied with the second type of atom. If the two types of atoms were randomly arranged the structure would be fcc. Derivative structures are ordered variants of a parent structure and are usually low temperature phases, since their configuration entropy is lower than that of the disordered fcc alloy parent phase. On atomic ordering, the symmetry of the structure decreases. For the case of fcc to $L1_0$, the decrease is in both

* Corresponding author. Address: Department of Physics, 5000 Forbes Ave., Carnegie Mellon University, Pittsburgh, PA 15213, United States. Tel.: +1 412 268 3135; fax: +1 412 268 3113.

E-mail address: mtanase@andrew.cmu.edu (M. Tanase).

¹ Present address: Department of Physics, Colorado State University, Fort Collins, CO 80523, United States.

² Present address: Advanced Microsensors Inc., Shrewsbury, MA 01545, United States.

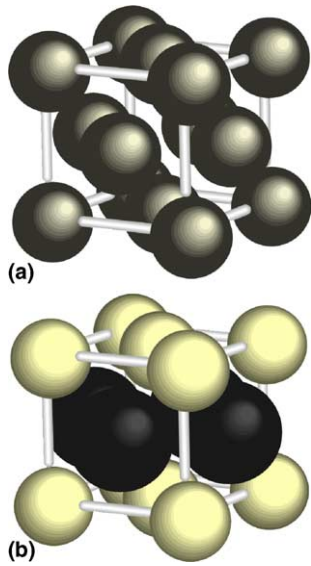


Fig. 1. (a) The disordered fcc unit cell. All sites have equal occupation probability of the two (or more) atoms of the alloy and (b) the L1₀ structure showing the alternating stacking of (001) planes.

translational symmetry and point group symmetry; see below for further discussion.

There are several ways of denoting the L1₀ structure. The Strukturbericht designation L1₀ is that given in the “Structure Reports” series of the early 20th century [1]. The prototype structure is CuAu I. The prototype is an actual phase that is either the first to be discovered or is an important phase with the structure that it denotes. Pearson [2] has combined Bravais lattice information and unit cell information in a notation which lists the crystal system (*c* for cubic, *t* for tetragonal, etc.), the Bravais Lattice (*P* for primitive, *F* for face centered, etc.) with the number of atoms in the unit cell. For the L1₀ structure the Pearson symbol is either tP4 (if the unit cell shown in Fig. 1b is used) or tP2 (if the smaller unit cell with lattice parameters $c' = c$ and $a' = a\sqrt{2}/2$ is used). The space group of the L1₀ structure is *P4/mmm*.

An important crystallographic feature of the L1₀ structure is its *c/a* ratio. Since this structure is based on a cubic one, if we use the unit cell shown in Fig. 1, $c/a \approx 1$. For most structures *c/a* is less than one, TiAl being the well known exception. If the two atom unit cell is used, the *c/a* ratio is about $\sqrt{2}$. It should be pointed out that even if the values of *a* and *c* were equal, the symmetry of the unit cell is tetragonal since there is no threefold axis and only one fourfold axis (along the *c*-axis of the L1₀ structure). The ordering of the atoms on specific sites has lowered the overall symmetry of the structure.

Another important aspect of the structure is the number and type of near neighbors. Since the distortion is small we can say that in the L1₀ structure there are 12 near neighbors (along the $\langle 110 \rangle$ directions) and six next near neighbors (along the $\langle 100 \rangle$ directions) as in its par-

Table 1

Site symmetry and occupation^a for *P4/mmm* space group

Atoms	Wyckoff notation	Symmetry	<i>x</i>	<i>y</i>	<i>z</i>
Au	1(a)	<i>4/mmm</i>	0.0	0.0	0.0
	1(c)	<i>4/mmm</i>	0.5	0.5	0.0
Cu	2(e)	<i>mmm</i>	0.0	0.5	0.5
		<i>(4/mmm)</i>	0.5	0.0	0.5

^a Based on the four atom unit cell of Fig. 1b.

ent fcc structure. For the L1₀ structure, each atom has eight opposite near neighbors and 4 similar near neighbors. (The opposite near neighbor bonds have a slightly smaller distance than the same near neighbor bonds for $c/a < 1$). Each atom also has six similar next-near neighbors. For energy calculations it is necessary to include at least the second nearest neighbors, as there is at least one other structure with the same number and type of first neighbors, namely the A₂B₂ structure that has the space group $I\frac{4}{a}md$ [3].

The positions of the atoms in the unit cell are summarized in Table 1. For the *P4/mmm* space group the 2(e) sites in general do not have the full space group symmetry. However, in the case of the four atom unit cell of the L1₀ structure, both types of atoms do have the site symmetry of *4/mmm*. The unit cell shown in Fig. 1b is actually a base centered tetragonal one. However, since base centered tetragonal cells can be redrawn as primitive tetragonal cells, to keep the number of Bravais lattices to a minimum, it has been decided by the International Crystallography community to designate all lattices with base centered tetragonal unit cells as primitive cells.

3. Changes in symmetry and the formation of domains

The fcc to L1₀ disorder to order atomic transformation produces:

- translational domains (also called anti-phase domains) due to the lowering of the translational symmetry;
- orientational domains (also called variants or merohedral twins) due to a lowering of the point symmetry.

In addition, the paramagnetic to ferromagnetic transformation in magnetic L1₀ alloys produces magnetic domains.

4. Crystallographic domains

4.1. Translational domains

The translational symmetry decreases by a factor of two in going from the fcc structure to one of the struc-

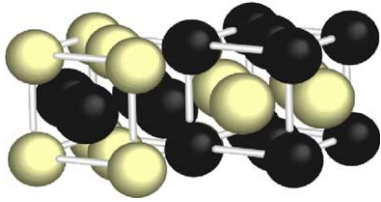


Fig. 2. The two translational domains of the $L1_0$ structure are displayed along with its higher energy anti-phase boundary.

tural domains of the $L1_0$ structure. This can be seen from Fig. 1 where there are four equivalent sites in the fcc structure per unit cell and two equivalent sites per unit cell in the $L1_0$ structure. This means that one half of the translational symmetry elements in the fcc structure are lost because of the atomic ordering. This loss in translational symmetry produces two translational or anti-phase domains per structure variant, as shown in Fig. 2. The interface between these domains has an energy associated with it, which is usually called the anti-phase boundary (APB) energy. These translational domains can be observed by transmission electron microscopy techniques. The local atomic bonding is disrupted at an APB and hence the local magnetocrystalline anisotropy energy is expected to vary there.

5. Crystallographic domains

5.1. Orientational domains (or variants)

Another type of domain which arises due to the decrease in symmetry during ordering is called a structural domain or variant. When the crystal is fcc it has three fourfold axes: after ordering to the $L1_0$ structure it has only one fourfold axis. This axis can be directed along any of the original cubic $\langle 100 \rangle$ axes, giving rise to three orientational or structural domains as shown in Fig. 3. These variants each can have two translational domains associated with them which means there can be six distinct domains in a materials undergoing the fcc to $L1_0$ transformation.

Once again the boundary between orientational domains is one of higher energy and also of a local change in the local magnetocrystalline anisotropy energy. The boundaries can be thought of as twin planes in that the structure on one side of the boundary twins into that on the other side of the boundary. These planes are of the type $\{101\}$ and in the fcc phase were mirror planes. These domains are also called merohedral twins. They are special twins, in that for other types of twins, such as those formed during annealing or deformation, the twin planes were not mirror planes before the formation of the twins.

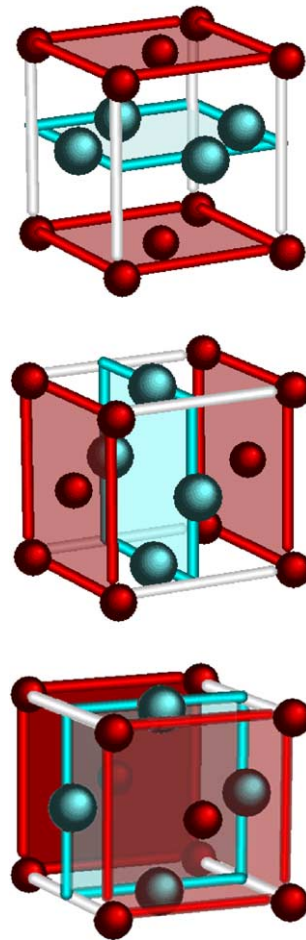


Fig. 3. The three orientational domains or variants that form when an fcc crystal orders to $L1_0$.

6. Ferromagnetic domains

Magnetic domains form because of the symmetry breaking that occurs during the magnetic ordering process. The arrangement of the domains is a result of minimizing some form of energy (magnetostatic, magnetoelastic, etc.).

When phases with the $L1_0$ structure are ferromagnetic the magnetization vector usually is along the $[001]$ axis of the crystal. Since magnetic fields have the symmetry of axial vectors (∞/mmm' in the Curie limiting group notation), the overall symmetry of the ferromagnetic crystal is decreased to $4/mmm'$ where the primed mirror planes represent the so-called magnetic mirror planes which take into account time reversal symmetry for the magnetic phase; see [4–7]. In terms of the classical space groups, the symmetry of the ferromagnetic $L1_0$ phase is $P4/m$, since the vertical mirror planes are lost on magnetic ordering [8].

The magnetization can be directed along either the $[001]$ or $[00\bar{1}]$ directions of the tetragonal phase

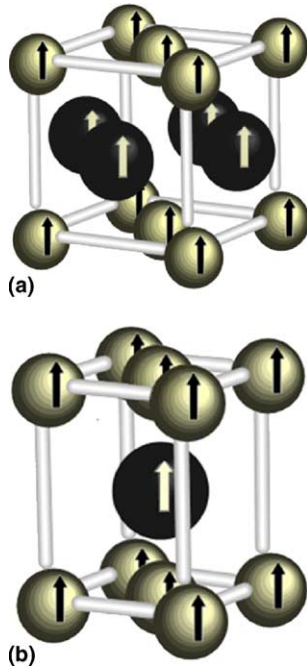


Fig. 4. Schematic of ferromagnetic $L1_0$ crystal with magnetic moment along $[001]$. On the left is the 4 atom unit cell (tP4) and on the right the 2 atom unit cell (tP2). The moments can also all be pointing down, meaning that there are two possible ferromagnetic domains. In this figure the axial magnetic vectors are indicated by polar vectors for ease of drawing.

(see Fig. 4). Thus there are two possible magnetic domains per structural domain when the phase is ferromagnetic. Since there are three possible structural domains and two translational domains per structural domain there are a total of twelve distinct domains of a ferromagnetic phase formed from the fcc structure with its magnetization along $\pm[001]$. The number of domains can also be obtained by dividing the order of the fcc paramagnetic group (96) divided by the order of the tetragonal ferromagnetic group (16) and multiplying the result by the change in translational symmetry on atomic ordering to the $L1_0$ structure (2).

7. Phase diagram and transformations

It has been pointed out [9] that most $L1_0$ phases form either by a peritectic transformation or from a high temperature disordered fcc phase. No congruently melting phase diagrams are known. Also, the single phase fields of $L1_0$ often have considerable width (large range of composition).

The phase diagrams for CoPt and FePt are given in Ref. [10]. The FePt $L1_0$ phase becomes stable at temperatures less than about 1300°C and the CoPt phase becomes stable at temperatures less than 825°C . The fcc to $L1_0$ transformation is a first order transformation after the Ehrenfest designation [11]. This can be deter-

mined from one of the criteria developed by Landau [12] and Lifshitz [13] and expanded on by Khachatryan [14] which, put in a simple form states that ratio of the order of the point groups (i.e. their index) of the disordered and ordered structures must be 2 if the phase transition is to have the possibility of being higher order. In the case of fcc to $L1_0$ the index is 3 (48, the order of the cubic point group, divided by 16 the order of the tetragonal point group). This means that at equilibrium the transition must be of first-order. It is for this reason that the diagrams show two phase fields adjacent to the single phase $L1_0$ field. These two phase fields are a necessary consequence of the first order character of the transition. It should be remembered that even though the transition is of first order, the reaction can occur homogeneously and continuously when the reaction temperature is away from the equilibrium phase boundary and below the instability temperature for the disordered alloy [15,16].

At temperatures near the solvus we expect the paramagnetic $L1_0$ phase to form by the nucleation and growth of highly ordered $L1_0$ phase. At larger undercoolings the reaction may occur continuously as discussed above. This means that it would start off with a small order parameter and gradually build up with time. At even larger undercoolings the transformation may occur in a massive like way which is similar to the transition designated “congruent ordering” by Khachatryan et al. [15]. Which of these types of transitions occurs will greatly affect the resulting microstructure of the material and hence its extrinsic properties. If an atomically disordered thin film of a $L1_0$ alloy is sputtered onto a substrate and is in biaxial tension it becomes tetragonal. Thus, the disordered tetragonal phase could atomically order via a higher order transition, according to the Landau rules. This may play a role in $L1_0$ thin film recording media.

8. Magnetic ordering

Both ferromagnetic and anti-ferromagnetic phases with the $L1_0$ structure are known to exist. It would be possible for a phase with the $L1_0$ structure to be ferromagnetic, but no unambiguous example could be found at the time this paper was written.

The ferromagnetic phases have their easy axis along the high symmetry axis of the structure, namely the $[001]$ direction. From the point of view of magnetic symmetry this lowers the point group of the paramagnetic $L1_0$ phase from $4/mmm1'$ (order 32 in magnetic symmetry) to $4/mmm'm'$ in the magnetic symmetry notation, which is of order 16. The lowering of the symmetry by a factor of two is the reason for the existence of two magnetic domains in uniaxial materials.

The ordering of the spins in anti-ferromagnetic phases is less certain. There are various possible arrangements, summarized in Fig. 5 [17].

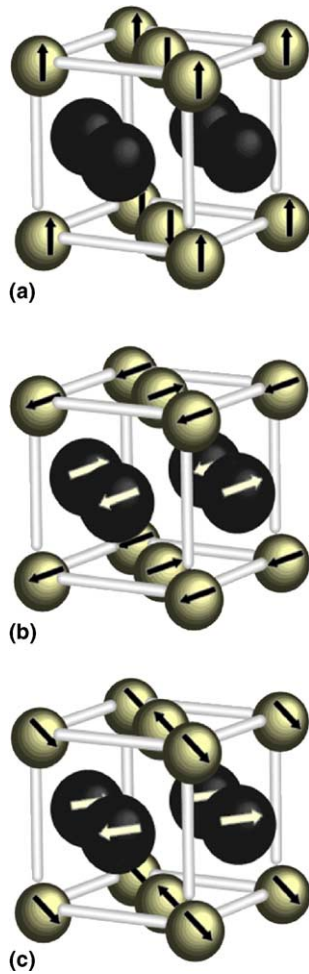


Fig. 5. Schematic of possible anti-ferromagnetic L₁₀ crystals. Again, in this figure the axial magnetic vectors are indicated by polar vectors for ease of drawing. In (a) the spins are along $\pm[001]$. In (b) the spins are along $\pm[100]$. In (c) the spins are along $\pm[110]$.

In Fig. 5a, only one of the elements is assumed to have a magnetic moment associated with it. The spins on a (001) plane are either directed up or down. The symmetry of this arrangement remains $4/mmm$, showing that there is only one antiferromagnetic domain with respect to the orientation of spins. However, in this case there are two translational domains which could in principle arise due to the loss of translational symmetry during the magnetic ordering. These domains will have very large interfacial energy because they will put parallel spins as near neighbors.

In Fig. 5b both elements are assumed to have a moment, but of different magnitude. Again the spins are thought to cancel in the (001) planes, but this time the direction of the spins is thought to be along the [100] direction of the unit cell. This lowers the symmetry to $mm'm'$ (the m being perpendicular to the [100]-axis). Thus in transforming from a paramagnetic L₁₀ phase to this antiferromagnetic structure the symmetry is lowered from $4/mmm1'$ (order 32 in magnetic symmetry) to

$mm'm'$ (order 8 in magnetic symmetry). Four domains are possible, two with their spins along the [100] direction and two with their spins along the [010] direction. Translational domains also exist for this structure, and once again will be of high interfacial energy.

Fig. 5c shows a third possibility of the alignment of the magnetic spins, this time along the face diagonals of the (001) planes. This orientation of the spins results in the same magnetic point group symmetry as in b. It should be pointed out that the near neighbor spins pointing to one another makes this structure highly energetic from the point of view of dipolar interaction energy.

9. Curie temperature

Magnetic ordering exists for both disordered fcc phase and ordered L₁₀ phase. It has been reported that the Curie temperature of the L₁₀ alloys can be affected by the atomic ordering transformation [18]. Wang et al. measured the Curie temperatures of disordered and ordered FePd alloys and found that the disordered (fcc) alloys have a Curie temperature about 30 K higher

Table 2
Measured Curie temperatures of FePd alloys

Composition	50% Pd		55%Pd		60%Pd	
Phase	fcc	L ₁₀	fcc	L ₁₀	fcc	L ₁₀
Curie T (K)	756	723	703	673	623	593

Values to ± 5 K.

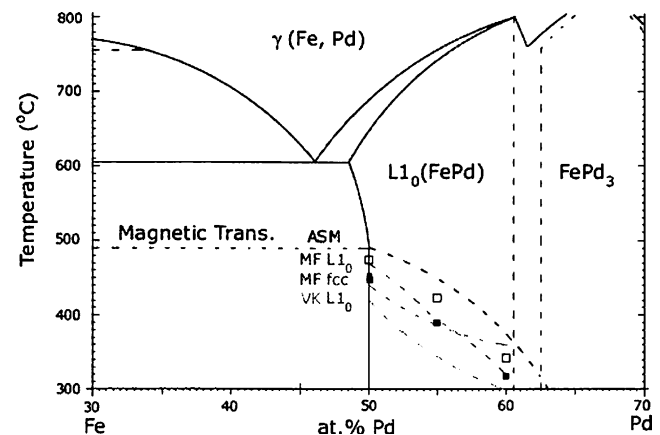


Fig. 6. FePd phase diagram shows the measured Curie temperatures for the fcc phase and the L₁₀ phase. Open squares are the measured Curie temperatures for the fcc phase. Solid squares are the measured Curie temperatures for the L₁₀ phase. The dotted curves are measured Curie temperatures for fcc and L₁₀ phases from [18,9,20] and [21].

than those of the ordered alloys [19]. Higher Curie temperature is closely related to the higher exchange coupling between the magnetic spins. For the same exchange coupling constant, the number of spin pairs (i.e. atomic near neighbors) determines the ferromagnetic exchange coupling strength. Table 2 and Fig. 6 show the results of the Curie temperatures measurement of FePd alloys [20]. From Fig. 6, it can be seen that increasing the Pd content from 50% to 60% decreases the Curie temperature for both fcc phase and L1₀ phase. This can be due to the decreasing number of the Fe–Fe and Fe–Pd nearest neighbors. Similarly, the atomic ordering transformation can also affect the atoms near neighbors and induces different Curie temperatures.

10. Concluding remarks

The crystallographic features of the L1₀ structure has several important aspects that affect its formation from the disordered fcc phase. In particular the breaking of the translational and orientational symmetry produces a variety of domains which in combination with the magnetic domains gives rise to a plethora of domain boundaries which all may affect the resulting magnetic properties. In this paper we reviewed the crystallography of the transformation and leave it to for another time to explore the specifics of the structure property relations in these ferromagnetic materials.

Acknowledgements

This work has been partially supported by SEAGATE Research, through the DSSC of CMU and the National Science Foundation, (grant DMR-9905725), through a Focused Research Group at CMU, Ohio State University and Rutgers University.

References

- [1] Strukturbericht, Zeitschrift für Kristallographie, Kristallgeometrie, Kristallphysik, Kristallchemie. Utrecht : A. Oosthoek; 1913ff.
- [2] Pearson WB. A handbook of lattice spacings and structures of metals and alloys, vol. 2. Oxford: Pergamon Press; 1967. p. 1.
- [3] Richards MJ, Cahn JW. Acta Metall. 1971;19:1263.
- [4] Opechowski W, Guccione R. Magnetic symmetry. Magnetism a treatise on modern theory and materials, vol. IIA. New York, NY: Academic Press; 1965. p. 105–65.
- [5] Cracknell AP. Magnetism in crystalline materials. Oxford: Pergamon Press; 1975.
- [6] Shaskolskaya S. Fundamentals of crystal physics. Moscow: Mir Publishers; 1982. Chapter VIII.
- [7] Joshua SJ. Symmetry principles and magnetic symmetry in solid state physics. Bristol: Adam Hilger; 1991.
- [8] Shen Y, Laughlin DE. Philos Mag Lett 1990;62(3):187.
- [9] Westbrook JH, Fleischer RL. Intermetallic compounds: principles and practice, vol. 1. New York, NY: John Wiley and Sons; 1995.
- [10] Massalski TB, Okamoto H. Binary alloy phase diagrams [CD-ROM]. Materials Park, OH: ASM International; 1996.
- [11] Ehrenfest, P. Verhandlingen der Koninklijke Akademie van Wetenschappen, vol. 36, Supplement no. 75b. Amsterdam: Communications from the Physical Laboratory of the University of Leiden; 1933. p. 153–7.
- [12] Landau LD. Sov Phys 1937;11:26. p 545.
- [13] Lifshitz EM. Fiz Zh 1942;7:61. p 251.
- [14] Khachatryan AG. Theory of structural transformations in solids. New York, NY: John Wiley and Sons; 1983.
- [15] Khachatryan AG, Lindsey TF, Morris JW. Metall Trans 1988;19A:249.
- [16] Soffa WA, Laughlin DE. Acta Metall 1989;37:3019.
- [17] Landolt-Börnstein: numerical data and functional relationships in science and technology, New Series vol. III 6 eds. Hellwege KH, Hellwege AM, vol. III 19a, 19c, ed. Wijn HPJ. New York: Springer-Verlag; 1988.
- [18] Fallot M. Les alliages du fer avec les métaux de la famille du platine. Ann Phys 1938;10:291.
- [19] Wang L. Atomic ordering, magnetic domain structure and magnetic properties of L1₀ type ferromagnets. Phd Thesis, Carnegie Mellon University, Pittsburgh, PA; 2004.
- [20] Wang L, Fan Z, Roy AG, Laughlin DE. J Appl Phys 2004;95:7483.
- [21] Kuprina VV, Grigor'ev AT. The iron–palladium system. Russ J Inorg Chem 1959;4:297.